Title

Phase-variance optical coherence tomography: a technique for noninvasive angiography.

Journal

Ophthalmology, 121(1)

ISSN

0161-6420

Authors

Schwartz, Daniel M
Fingler, Jeff
Kim, Dae Yu
et al.

Publication Date

2014

DOI

10.1016/j.ophtha.2013.09.002

Peer reviewed

Phase-Variance Optical Coherence Tomography

A Technique for Noninvasive Angiography

Daniel M. Schwartz, MD,[1] Jeff Fingler, PhD,[2] Dae Yu Kim, PhD,[2,3] Robert J. Zawadzki, PhD,[3] Lawrence S. Morse, MD, PhD,[3] Susanna S. Park, MD, PhD,[3] Scott E. Fraser, PhD,[2] John S. Werner, PhD[3]

Purpose: Phase-variance optical coherence tomography (PV-OCT) provides volumetric imaging of the retinal vasculature without the need for intravenous injection of a fluorophore. We compare images from PV-OCT and fluorescein angiography (FA) for normal individuals and patients with age-related macular degeneration (AMD) and diabetic retinopathy.

Design: This is an evaluation of a diagnostic technology.

Participants: Four patients underwent comparative retinovascular imaging using FA and PV-OCT. Imaging was performed on 1 normal individual, 1 patient with dry AMD, 1 patient with exudative AMD, and 1 patient with nonproliferative diabetic retinopathy.

Methods: Fluorescein angiography imaging was performed using a Topcon Corp (Tokyo, Japan) (TRC-50IX) camera with a resolution of 1280 (H) × 1024 (V) pixels. The PV-OCT images were generated by software data processing of the entire cross-sectional image from consecutively acquired B-scans. Bulk axial motion was calculated and corrected for each transverse location, reducing the phase noise introduced from eye motion. Phase variance was calculated through the variance of the motion-corrected phase changes acquired within multiple B-scans at the same position. Repeating these calculations over the entire volumetric scan produced a 3-dimensional PV-OCT representation of the vasculature.

Main Outcome Measures: Feasibility of rendering retinal and choroidal microvasculature using PV-OCT was compared qualitatively with FA, the current gold standard for retinovascular imaging.

Results: Phase-variance OCT noninvasively rendered a 2-dimensional depth color-coded vasculature map of the retinal and choroidal vasculature. The choriocapillaris was imaged with better resolution of microvascular detail using PV-OCT. Areas of geographic atrophy and choroidal neovascularization imaged by FA were depicted by PV-OCT. Regions of capillary nonperfusion from diabetic retinopathy were shown by both imaging techniques; there was not complete correspondence between microaneurysms shown on FA and PV-OCT images.

Conclusions: Phase-variance OCT yields high-resolution imaging of the retinal and choroidal microvasculature that compares favorably with FA. *Ophthalmology 2014;121:180-187 © 2014 by the American Academy of Ophthalmology.*

Since the initial studies by Novotny and Alvis more than 50 years ago, fluorescein angiography (FA) remains the gold standard for retinovascular imaging.[1,2] An estimated 1 million FA studies are performed annually in the United States.[3] Although FA has obvious value in revealing fine details of the microvasculature, it requires an intravenous injection and a skilled photographer and is time-consuming. Minor side effects such as nausea, vomiting, and multiple needle sticks in patients with challenging venous access are not uncommon.[4] Because fluorescein leaks readily through the fenestrations of the choriocapillaris, it is not suitable for showing the anatomy of this important vascular layer that supplies the outer retina. Indocyanine green angiography provides improved visualization of choroidal anatomy because this dye is more extensively protein bound than fluorescein and does not leak into the extravascular space as readily.[5] Furthermore, it fluoresces at a longer wavelength than fluorescein and imaging can take place through pigment and thin layers of blood. Nevertheless, indocyanine green imaging fails to depict the fine anatomic structure of the choriocapillaris.[6,7]

Since the introduction of optical coherence tomography (OCT) in 1991, it has become an indispensable clinical imaging tool.[8,9] Use of spectral-domain OCT (SD-OCT) enables high-resolution imaging of retinal morphology that is nearly comparable to histologic analysis. Despite the rapid evolution of OCT imaging, SD-OCT does not provide adequate visualization of retinal and choroidal microvasculature. Thus, as clinicians, we are often compelled to order both OCT and FA in patients with common retinovascular diseases, such as age-related macular degeneration (AMD), diabetic retinopathy, and retinovascular occlusions.

There has been increased interest in using data generated during SD-OCT imaging to generate angiographic images of

ISSN 0161-6420/14/$ - see front matter
http://dx.doi.org/10.1016/j.ophtha.2013.09.002

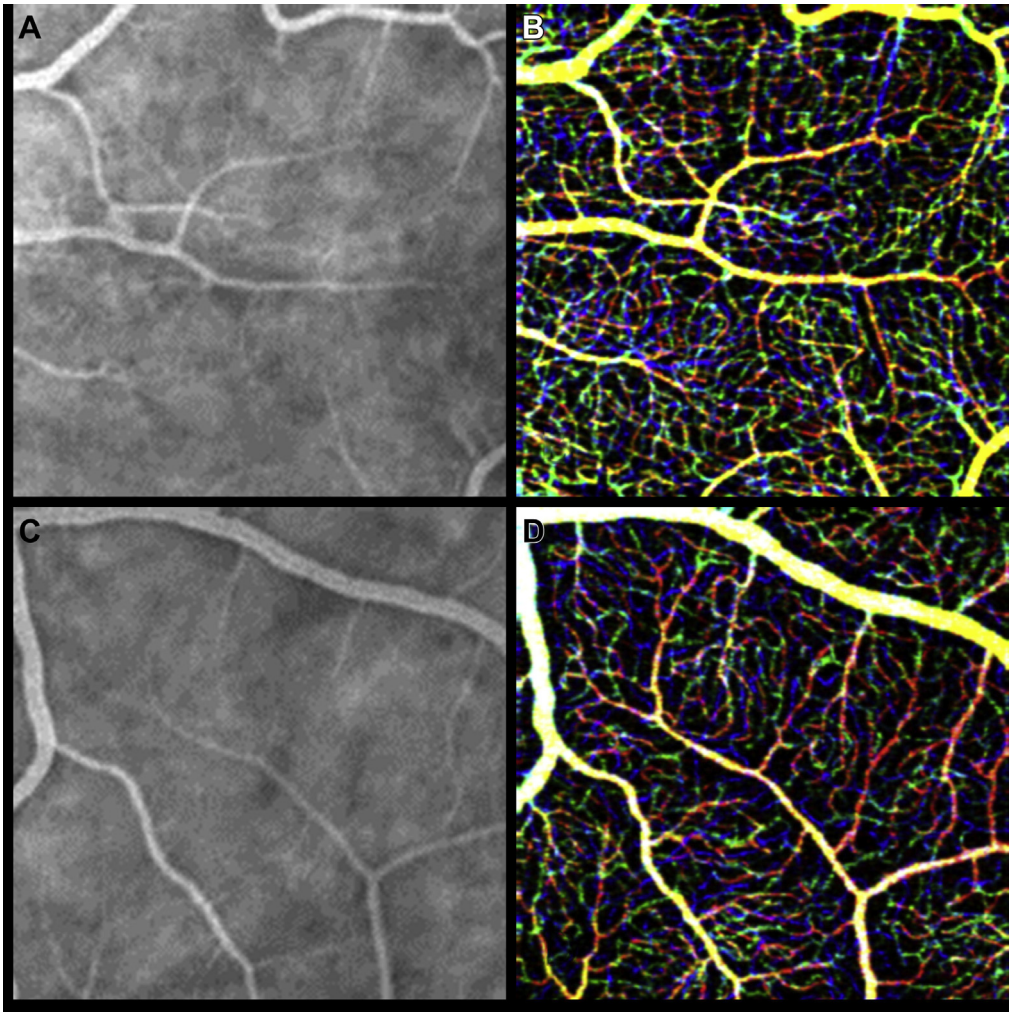

Figure 1. Comparison between fluorescein angiography (FA) (**A, C**) and phase-variance optical coherence tomography (PV-OCT) (**B, D**) over 1.5×1.5 mm^2 areas in parafovea (*top*: 8° nasal eccentricity, *bottom*: 8° temporal and superior eccentricity) of a 60-year-old normal subject. Phase-variance OCT is red-green-blue color coded to represent the depth imaging, which is not captured in FA data sets. *Red* is the most superficial capillary bed, *green* is the intermediate capillary plexus, and *blue* is the deeper capillary network. Larger-diameter vessels are *yellowish* because of positioning in both superficial and intermediate layers.

the fundus. These angiograms are implemented non-invasively without injection of fluorescent dye. Fingler et al[10–12] and Kim et al[13,14] have used phase-variance OCT (PV-OCT), also called phase-variance OCT, to image retinal microvasculature. This technique uses software processing of data normally acquired, but not used, during SD-OCT imaging. With a different scanning protocol than found in commercial instruments, PV-OCT identifies regions of motion between consecutive B-scans that are contrasted with less mobile regions. In the retina and choroid, the regions with motion correspond to the vasculature; these vessels are readily differentiated from other retinal tissues that are relatively static. An alternative method to acquire images of the retinal microvasculature is Doppler OCT, which measures the change in scatterer position between successive depth scans and uses this information to calculate the flow component parallel to the imaging direction (called axial flow).[15–17] Doppler OCT has been used to image large axial flow in the retina, but without dedicated scanning protocols[18] this technique is limited in cases of slow flow or flow oriented transverse to the imaging direction. Because this technique depends on measuring motion changes between successive depth scans, as imaging speed improvements continue for SD-OCT systems, the scatterers have less time to move between measurements and the slowest motions become obscured by noise. This reduces the visualization capabilities of typical Doppler OCT techniques. In contrast, PV-OCT will be able to achieve the same time separations between phase measurements with increased SD-OCT imaging speeds, maintaining the demonstrated ability to visualize fast blood vessel and slow microvascular flow independently of vessel orientation.

Several groups in recent years have developed OCT imaging methods to push beyond conventional Doppler OCT imaging limitations. Some approaches involve increasing the flow contrast through hardware

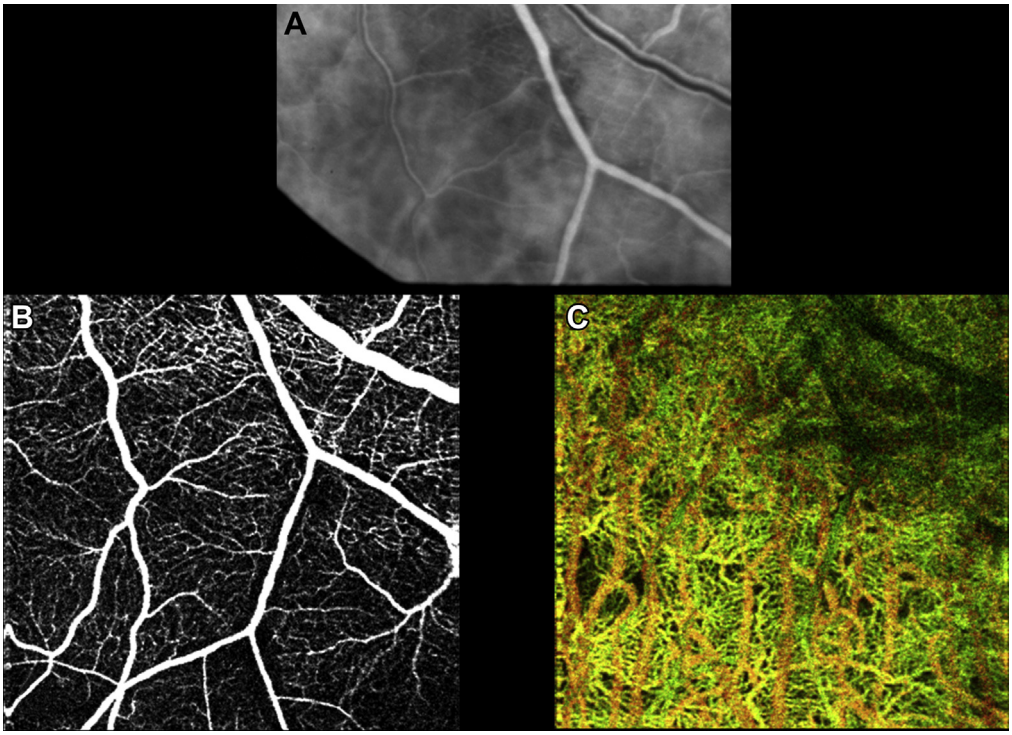

Figure 2. Comparison of fluorescein angiography (FA) and phase-variance optical coherence tomography (PV-OCT) imaging of retinal and choroidal vasculature just outside the inferotemporal arcade. **A,** Fluorescein angiography in laminar phase. En face projection of PV-OCT (**B**) shows retinal vasculature of the same region. The color-coded image (**C**) shows choroidal vasculature: superficial choroidal vessels (choriocapillaris, Sattler's layer) in *green* and larger choroidal vessels (Haller's layer) in *orange*. Notice that shadows of retinal vasculature generate artifacts in *black* in the *upper right* area in (**C**).

modifications of SD-OCT machines, such as in 2-beam scanning,[19,20] or producing a heterodyne frequency for extracting flow components.[21] Other investigators have used nonconventional scanning patterns[22] or repeated B-scan acquisitions,[23,24] such as used in PV-OCT to increase the time separation between phase measurements and enhance Doppler flow contrast of microvascular flow. In addition to phase-based contrast techniques to visualize vasculature, intensity-based visualization of microvasculature has been developed for OCT using segmentation,[25] speckle-based temporal changes,[26,27] decorrelation-based techniques,[28] and contrast based on both phase and intensity changes.[29] Each of these methods has varying capabilities in regard to microvascular visualization, noise levels, and artifacts while imaging retinal tissues undergoing typical motion during acquisition. Some of the noise and artifact limitations can be overcome with selective segmentation of the volumetric data or increased statistics through longer imaging times, but further analysis is required to be able to compare all of the visualization capabilities from all these different systems.

We show the preliminary capabilities of PV-OCT to image retinal and choroidal microvasculature in normal subjects and patients with AMD and diabetic retinopathy.

Methods

The tenets of the Declaration of Helsinki were observed, and written informed consent approval by the institutional review board was obtained. For FA imaging, each subject's pupils were dilated with a combination of 1% tropicamide and 2.5% phenylephrine. Sodium fluorescein 10% in water (500 mg/5 ml) was injected intravenously, followed by a flush of normal saline. Fundus FA images were acquired with a Topcon Corp (Tokyo, Japan) (TRC-50IX) camera with a resolution of 1280 (H) × 1024 (V) pixels.

Two different OCT instruments were used in the acquisition of PV-OCT data presented. The primary system was a high-speed (125-kHz A-scan rate) SD-OCT system constructed at the University of California, Davis that acquired in vivo human retinal images with scanning areas of 1.5 × 1.5 mm^2 or 3 × 3 mm^2.[13] Figures 1, 2, 3, 5, and 6 were acquired with this 125-kHz OCT system. Another system operating at 25 kHz at the University of California, Davis was used to acquire retinal scanning areas of 1 × 1 mm^2.[12] We used this system to acquire Figure 4. A bite-bar and a forehead rest were used to stabilize head position for both systems. The image acquisition time of each PV-OCT volumetric scan was less than 5 seconds for each system.

Optical Coherence Tomography Instrumentation

A schematic of the SD-OCT instruments used in this study has been reported.[12,13] The OCT systems operated at a center wavelength of 855 nm and with a full-width-half-maximum of 75 nm, resulting in an axial resolution of approximately 4.5 μm in tissue and focused in the retina with an approximate lateral resolution of 15 μm. Scanning protocols used to acquire the PV-OCT data were volumetric scans composed of BM-scans (B-M-mode scans), which are a series of sequential B-scans acquired over the same spatial region in the retina. The phase differences between sequential B-scans within each BM-scan were extracted for the phase-variance contrast calculation. The spacing between consecutive A-scans and BM-scans for the scan patterns presented ranged from as small as 3 μm for the densely sampled scans to as large as

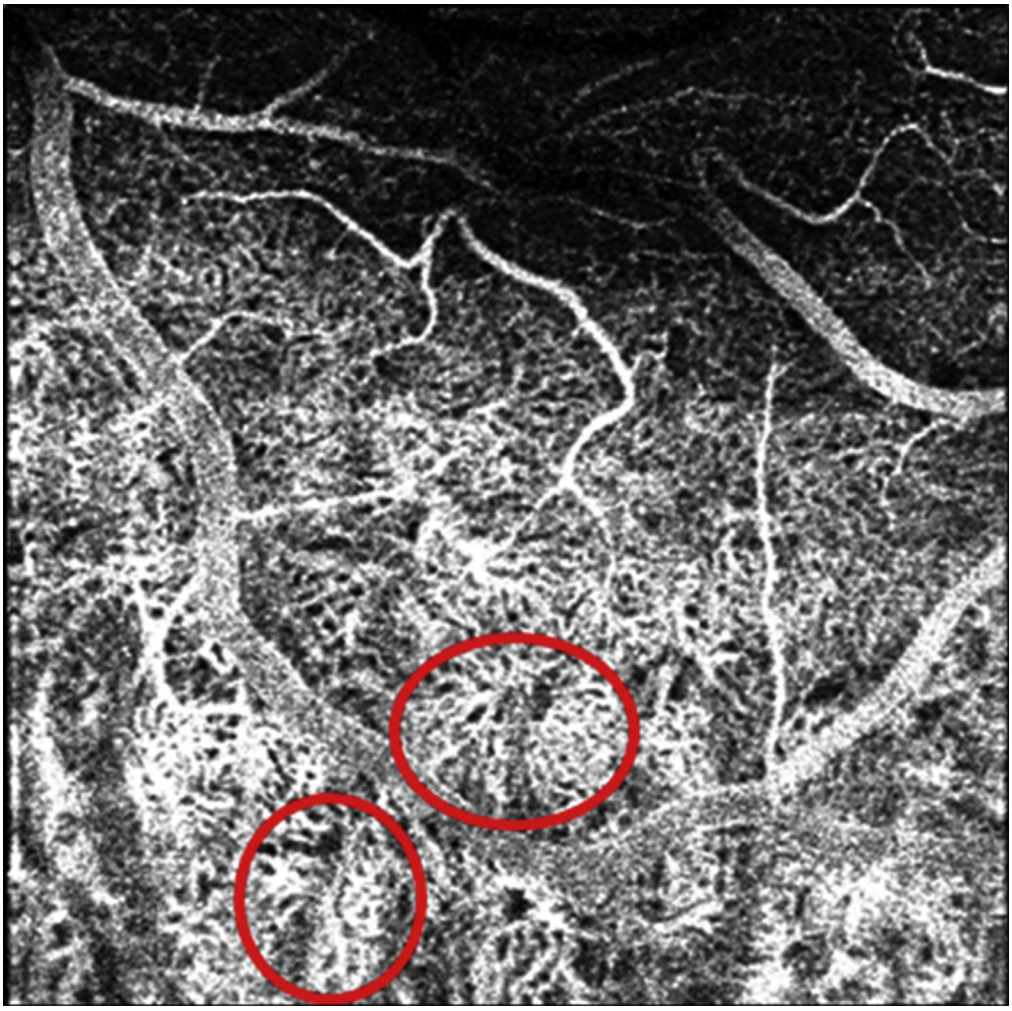

Figure 3. Phase-variance optical coherence tomography (PV-OCT) showing depth imaging of retinal and choroidal vasculature. Putative choriocapillaris lobules are circled in *red*.

15 μm for scans with the lowest sampling density. Graphic programming–based software (LabVIEW; National Instruments, Austin, TX) was used to acquire and process PV-OCT data sets.

Phase-Variance Method

Phase changes were calculated for the entire cross-sectional image from consecutively acquired B-scans. Bulk axial motion was calculated and corrected for each transverse location, reducing the phase noise introduced from eye motion. Phase variance was calculated through the variance of the motion-corrected phase changes acquired within a BM-scan. Intensity thresholding of the average OCT intensity image was used to create a mask for the PV-OCT image that removes contributions of phase noise caused by low signal-to-noise regions. Repeating these calculations over the entire volumetric scan produces a 3-dimensional PV-OCT representation of the vasculature. Further details regarding BM-scans and the phase variance contrast processing have been reported.[10,12]

Image Processing

The volumetric data set processed by the phase-variance contrast method was segmented manually from the nerve fiber layer to the outer plexiform layer for characterization of the retinal circulation. The choroidal vasculature was imaged by segmenting the data deep to the retinal pigment epithelium layer. Pseudo-color coding of depth position showed distinct locations of vascular networks. Its en face projection view produced a 2-dimensional depth color-coded vasculature map.

Results

Normal Subjects: Comparison of Retinal and Choroidal Vasculature Imaged by Fluorescein Angiography and Phase-Variance Optical Coherence Tomography

Figure 1 shows a comparison between FA and PV-OCT imaging of the retinal vasculature along the inferotemporal arcade from a 60-year-old healthy man. Color coding of the PV-OCT images delineates capillary architecture of different retinal depths. This level of resolution is not depicted using conventional FA where microvascular resolution is partially "washed out" by background choroidal fluorescence.

Figure 2 demonstrates the capability of PV-OCT to image the choroid. Fluorescein angiography (Fig 2A) is shown of the same region for comparison with projection (Fig 2B) of retinal vessels from PV-OCT data. As shown in Figure 1, PV-OCT imaging of

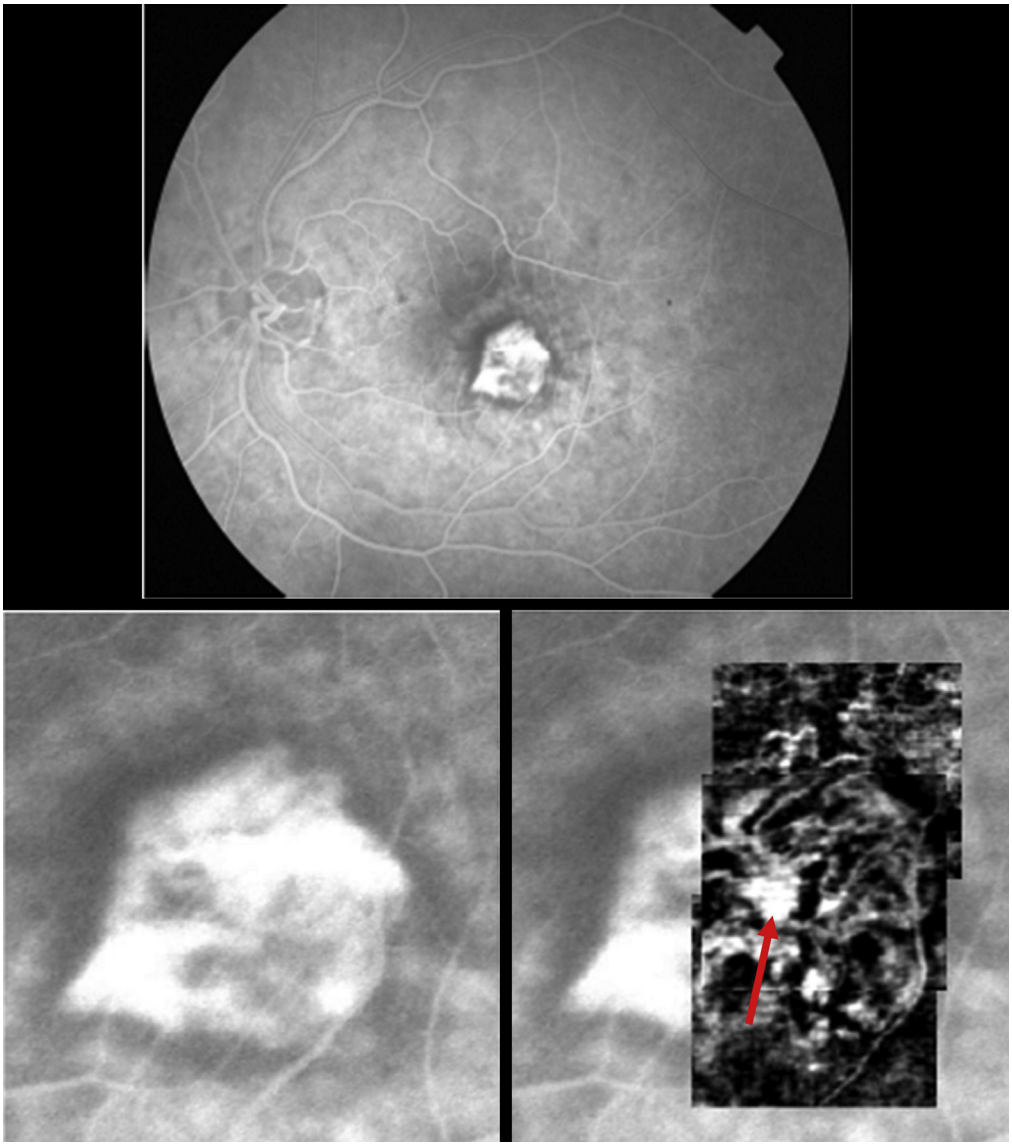

Figure 4. Wet age-related macular degeneration (AMD) with subfoveal choroidal neovascularization (CNV). *Top* shows early laminar flow transit fluorescein angiography (FA) of subfoveal classic CNV. *Lower left* shows magnification of FA, zoomed into region of CNV. *Lower right* is overlay of phase-variance optical coherence tomography (PV-OCT) montage of the subfoveal CNV. Note cartwheel shape of multiple vascular spokes emanating from probable central feeder vessel (*red arrow*). Phase-variance OCT data are based on consecutive B-scans, each acquired with 25-kHz University of California, Davis system over 1×1 mm^2.

the retinal vasculature compares favorably to resolution by FA of the same region. The depth-coded vasculature (Fig 2C) of the choroid is shown by PV-OCT, where overlying retinal vessels are shown as shadows. Superficial vessels of the choriocapillaris and Sattler's layer are shown, as are deeper, larger choroidal vessels of Haller's layer.

Figure 3 shows another region of choroidal imaging from the same individual. Note the fine structure of apparent choroidal lobules (circled) with feeding arterioles at its center and radiating capillaries extending toward draining venules.

Dry and Wet Age-Related Macular Degeneration

Figure 4 shows an 85-year-old man with subfoveal choroidal neovascularization (CNV); vision is 20/100. Comparative imaging with FA and PV-OCT is shown. On the right, the CNV imaged with PV-OCT is overlaid over the high magnification FA. The ability of PV-OCT to capture the fine vascular detail of this classic CNV is evident. The enhanced clarity of microvascular detail revealed by PV-OCT compared with FA is in part because PV-OCT does not detect a breakdown of the blood retinal barrier. Fluorescein at this stage of the angiogram leaks from CNV and extravascular dye obscures fine microvasculature.

Figure 5 shows a case of AMD with geographic atrophy (GA) in a 61-year-old woman with vision of 20/60 in the left eye. A red-free photograph shows 2 regions of well-delineated GA, 1 centered just inferonasal to fixation and the other smaller area just inferotemporal to the fovea. Early-phase FA displays the regions of GA and adjacent areas of patchy atrophy. The 2 lower frames compare high magnification views by FA and PV-OCT. The PV-OCT image is

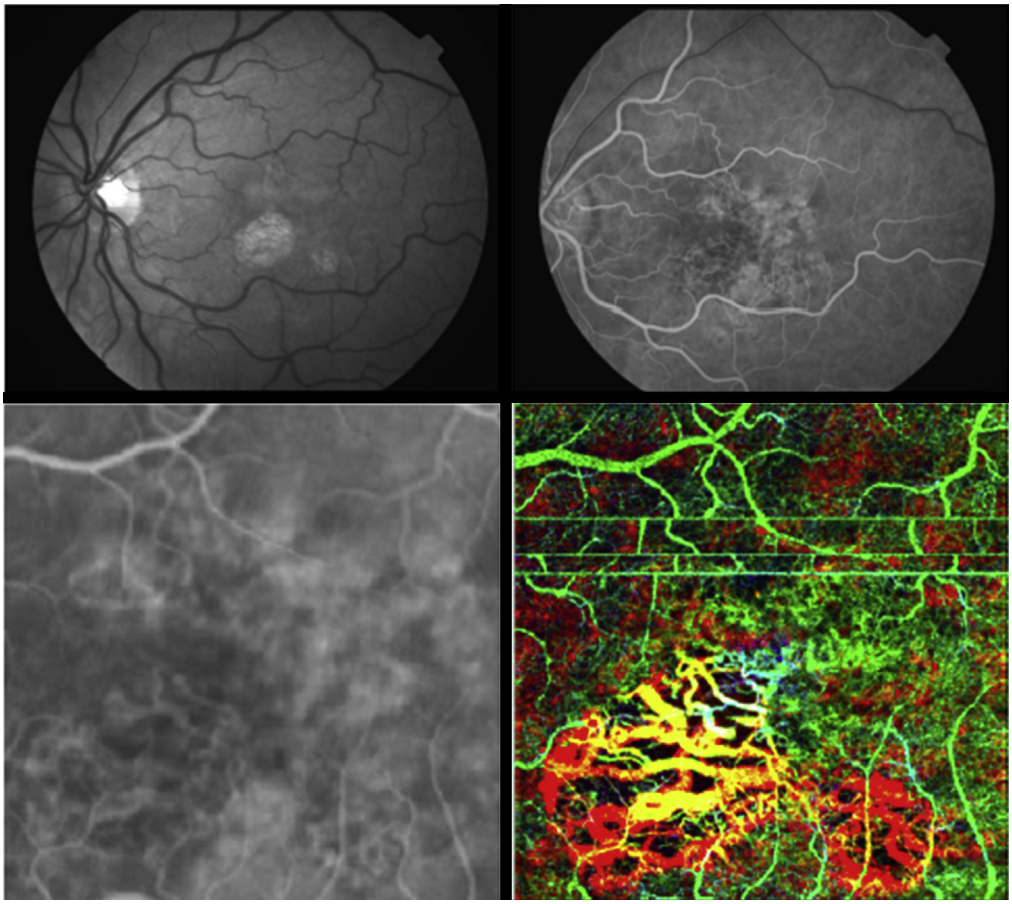

Figure 5. A 61-year-old woman with dry age-related macular degeneration (AMD). *Top left* shows red-free photograph; *top right* is laminar flow phase of fluorescein angiography (FA). *Lower left* is high magnification FA image of foveal region; *lower right* shows a 3 × 3 mm phase-variance optical coherence tomography (PV-OCT) depth image of same region, color coded. (*Green* is superficial/anterior choroidal region, which includes horizontal motion artifacts. *Yellow* is deeper into choroid, and *red* is the deepest imaging plane.) All slices are fixed distances relative to the anterior surface of retina.

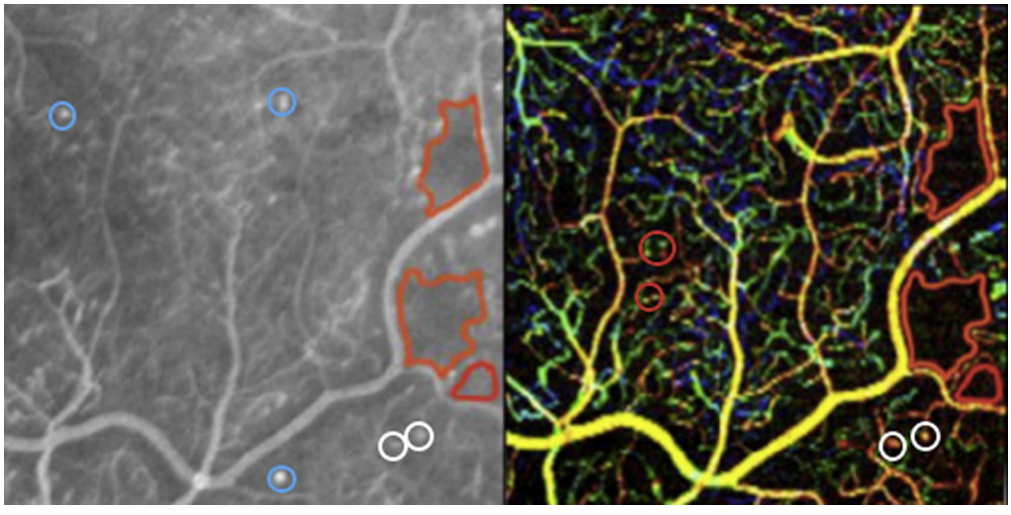

Figure 6. View of temporal retina in a patient with proliferative diabetic retinopathy. Fluorescein angiography (FA) on *left* shows multiple microaneurysms; regions of capillary nonperfusion are outlined in red. A 3 × 3 mm phase-variance optical coherence tomography (PV-OCT) image on *right* shows similarly shaped regions of capillary nonperfusion outlined in red. Although some microaneurysms are shown by FA and PV-OCT (*white circles*), others are only shown in the FA image (*blue circles*) or PV-OCT (*red circles*).

color coded for depth; the areas of GA show large choroidal vessels and loss of the overlying superficial choriocapillaris.

Diabetic Retinopathy

Figure 6 shows a case of nonproliferative diabetic retinopathy with regions of capillary nonperfusion in a 29-year-old woman with type 1 diabetes for 17 years; vision is 20/25 in the left eye.

Although regions of capillary nonperfusion, delineated with red contours in the right side of Figure 6, are comparably imaged using PV-OCT, microaneurysms are generally more apparent in the FA. Some microaneurysms seen on FA are not imaged by PV-OCT, and conversely others are visible by PV-OCT, but less so by FA.

Discussion

We have shown the capability of PV-OCT to provide imaging comparable to FA in normal subjects and patients with AMD and diabetic retinopathy. Obtaining PV-OCT angiography does not require hardware alterations in current SD-OCT instruments; instead, software analysis of data acquired during routine SD-OCT imaging is further processed to yield angiographic images. Indeed, we have recently begun using a commercial SD-OCT platform to generate PV-OCT images. In contrast to FA, PV-OCT angiographic imaging is accomplished noninvasively. Because it is technically easier to perform OCT imaging than FA, which requires a skilled photographer, PV-OCT is obtained with minimal training.

Phase-variance OCT angiographic imaging is based on the contrast of moving versus more static tissues. Therefore, it is particularly well suited to display the fine structure of the capillary networks. Three-dimensional imaging with PV-OCT generates high-resolution depth imaging of retinal and choroidal vasculature using SD-OCT. Although angiographic imaging with PV-OCT seems to compare favorably to conventional FA, processing methods currently used in PV-OCT do not reveal vascular leakage. Therefore, FA would be preferable for imaging cases of central serous retinopathy where detection of a leakage site is used to guide laser therapy.

Imaging of microaneurysms in diabetic retinopathy does not show exact correspondence between FA and PV-OCT. Although some microaneurysms were shown by both imaging techniques, others were shown by only FA or PV-OCT. The reason for this is probably related to the plane of imaging by PV-OCT. Although FA images all retinal and choroidal vasculature simultaneously, PV-OCT imaging is depth-based (volumetric). Thus, microvascular alterations seen on FA could be detected by PV-OCT if other retinal planes were imaged. We are currently exploring this possibility as more patients are imaged. Accurate depiction of microaneurysms by PV-OCT is important if it were to be used as an alternative to FA for guiding laser therapy.

How would PV-OCT be used in clinical practice? Because images are obtained with standard SD-OCT imaging, PV-OCT imaging of diabetic patients might allow improved characterization of disease severity. Specifically, the extent of retinal capillary nonperfusion could be characterized better than by ophthalmoscopy alone. Although this also could be achieved using FA, this is not commonly done because of the cost and complexity of this test. Furthermore, although not demonstrated in this article, PV-OCT could be used to follow patients with high-risk drusen as a means to detect early CNV, perhaps before it becomes symptomatic and causes visual loss. Were this the case, then anti-vascular endothelial growth factor therapy might be initiated earlier in the course of wet AMD with possible preservation of better vision. The ability of PV-OCT to characterize choroidal microvasculature also is intriguing. Imaging could improve our understanding of GA[30] and how alterations in the choriocapillaris might also contribute to the development of wet AMD.[31]

In conclusion, because of its simplicity, noninvasive character, and apparent improved ability to render microvascular detail, PV-OCT may be used increasingly as an alternative to FA.

References

1. Alvis D. Happy 50th birthday [letter]. Ophthalmology 2009; 116:2259.
2. Marmor MF, Ravin JG. Fluorescein angiography: insight and serendipity a half century ago. Arch Ophthalmol 2011;129: 943–8.
3. Swanson EA, Huang D. Ophthalmic OCT reaches $1 billion per year. Retin Physician 2011;8:45, 58, 59, 62.
4. Lipson BK, Yannuzzi LA. Complications of intravenous fluorescein injections. Int Ophthalmol Clin 1989;29:200–5.
5. Owens SL. Indocyanine green angiography. Br J Ophthalmol 1996;80:263–6.
6. Pauleikhoff D, Spital G, Radermacher M, et al. A fluorescein and indocyanine green angiographic study of choriocapillaris in age-related macular disease. Arch Ophthalmol 1999;117: 1353–8.
7. Flower RW, Fryczkowski AW, McLeod DS. Variability in choriocapillaris blood flow distribution. Invest Ophthalmol Vis Sci 1995;36:1247–58.
8. Huang D, Swanson EA, Lin CP, et al. Optical coherence tomography. Science 1991;254:1178–81.
9. van Velthoven ME, Faber DJ, Verbraak FD, et al. Recent developments in optical coherence tomography for imaging the retina. Prog Retin Eye Res 2007;26:57–77.
10. Fingler J, Schwartz D, Yang C, Fraser SE. Mobility and transverse flow visualization using phase variance contrast with spectral domain optical coherence tomography. Opt Express [serial online] 2007;15:12636–53. Available at: http://www.opticsinfobase.org/oe/abstract.cfm?uri=oe-15-20-12636. Accessed August 24, 2013.
11. Fingler J, Readhead C, Schwartz DM, Fraser SE. Phase-contrast OCT imaging of transverse flows in the mouse retina and choroid. Invest Ophthalmol Vis Sci 2008;49:5055–9.
12. Fingler J, Zawadzki RJ, Werner JS, et al. Volumetric microvascular imaging of human retina using optical coherence tomography with a novel motion contrast technique. Opt Express [serial online] 2009;17:22190–200. Available at: http://www.opticsinfobase.org/oe/abstract.cfm?uri=oe-17-24-22190. Accessed August 24, 2013.
13. Kim DY, Fingler J, Werner JS, et al. In vivo volumetric imaging of human retinal circulation with phase-variance optical coherence tomography. Biomed Opt Express [serial online] 2011;2:1504–13. Available at: http://www.opticsinfobase.org/boe/fulltext.cfm?uri=boe-2-6-1504&id=213832. Accessed August 24, 2013.

14. Kim DY, Fingler J, Zawadzki RJ, et al. Noninvasive imaging of the foveal avascular zone with high-speed, phase-variance optical coherence tomography. Invest Ophthalmol Vis Sci 2012;53:85–92.
15. White B, Pierce M, Nassif N, et al. In vivo dynamic human retinal blood flow imaging using ultra-high-speed spectral domain optical coherence tomography. Opt Express [serial online] 2003;11:3490–7. Available at: http://www.opticsinfobase.org/oe/abstract.cfm?uri=oe-11-25-3490. Accessed August 24, 2013.
16. Leitgeb RA, Schmetterer L, Hitzenberger CK, et al. Real-time measurement of in vitro flow by Fourier-domain color Doppler optical coherence tomography. Opt Lett 2004;29:171–3.
17. Tao YK, Kennedy KM, Izatt JA. Velocity-resolved 3D retinal microvessel imaging using single-flow imaging spectral domain optical coherence tomography. Opt Express [serial online] 2009;17:4177–88. Available at: http://www.opticsinfobase.org/oe/abstract.cfm?uri=oe-17-5-4177. Accessed August 24, 2013.
18. Grulkowski I, Gorczynska I, Szkulmowski M, et al. Scanning protocols dedicated to smart velocity ranging in spectral OCT. Opt Express [serial online] 2009;17:23736–54. Available at: http://www.opticsinfobase.org/oe/abstract.cfm?uri=oe-17-26-23736. Accessed August 24, 2013.
19. Zotter S, Pircher M, Torzicky T, et al. Visualization of microvasculature by dual-beam phase-resolved Doppler optical coherence tomography. Opt Express [serial online] 2011;19:1217–27. Available at: http://www.opticsinfobase.org/oe/fulltext.cfm?uri=oe-19-2-1217&id=209402. Accessed August 24, 2013.
20. Makita S, Jaillon F, Yamanari M, et al. Comprehensive in vivo micro-vascular imaging of the human eye by dual-beam-scan Doppler optical coherence angiography. Opt Express [serial online] 2011;19:1271–83. Available at: http://www.opticsinfobase.org/oe/fulltext.cfm?uri=oe-19-2-1271&id=209407. Accessed August 24, 2013.
21. Wang RK, Jacques SL, Ma Z, et al. Three dimensional optical angiography. Opt Express [serial online] 2007;15:4083–97. Available at: http://www.opticsinfobase.org/oe/abstract.cfm?uri=oe-15-7-4083. Accessed August 24, 2013.
22. Braaf B, Vermeer KA, Vienola KV, de Boer JF. Angiography of the retina and the choroid with phase-resolved OCT using interval-optimized backstitched B-scans. Opt Express [serial online] 2012;20:20516–34. Available at: http://www.opticsinfobase.org/oe/fulltext.cfm?uri=oe-20-18-20516&id=240889. Accessed August 24, 2013.
23. Kurokawa K, Sasaki K, Makita S, et al. Three-dimensional retinal and choroidal capillary imaging by power Doppler optical coherence angiography with adaptive optics. Opt Express [serial online] 2012;20:22796–812. Available at: http://www.opticsinfobase.org/oe/fulltext.cfm?uri=oe-20-20-22796&id=242390. Accessed August 24, 2013.
24. Braaf B, Vienola KV, Christy K, et al. Real-time eye motion correction in phase-resolved OCT angiography with tracking SLO. Biomed Opt Express [serial online] 2013;4:51–65. Available at: http://www.opticsinfobase.org/boe/fulltext.cfm?uri=boe-4-1-51&id=246986. Accessed August 24, 2013.
25. Schmoll T, Singh AS, Blatter C, et al. Imaging of the parafoveal capillary network and its integrity analysis using fractal dimension. Biomed Opt Express [serial online] 2011;2:1159–68. Available at: http://www.opticsinfobase.org/boe/fulltext.cfm?uri=boe-2-5-1159&id=211741. Accessed August 24, 2013.
26. Mariampillai A, Leung MK, Jarvi BA, et al. Optimized speckle variance OCT imaging of microvasculature. Opt Lett 2010;35:1257–9.
27. Motaghiannezam R, Fraser S. Logarithmic intensity and speckle-based motion contrast methods for human retinal vasculature visualization using swept source optical coherence tomography. Biomed Opt Express [serial online] 2012;3:503–21. Available at: http://www.opticsinfobase.org/boe/fulltext.cfm?uri=boe-3-3-503&id=227627. Accessed August 24, 2013.
28. Jia Y, Tan O, Tokayer J, et al. Split-spectrum amplitude-decorrelation angiography with optical coherence tomography. Opt Express [serial online] 2012;20:4710–25. Available at: http://www.opticsinfobase.org/oe/fulltext.cfm?uri=oe-20-4-4710&id=227624. Accessed August 24, 2013.
29. Liu G, Chou L, Jia W, et al. Intensity-based modified Doppler variance algorithm: application to phase instable and phase stable optical coherence tomography systems. Opt Express [serial online] 2011;19:11429–40. Available at: http://www.opticsinfobase.org/oe/fulltext.cfm?uri=oe-19-12-11429&id=214327. Accessed August 24, 2013.
30. Kim DY, Fingler J, Zawadzki RJ, et al. Optical imaging of the chorioretinal vasculature in the living human eye. Proc Natl Acad Sci U S A 2013;110:14354–9.
31. Bhutto I, Lutty G. Understanding age-related macular degeneration (AMD): relationships between the photoreceptor/retinal pigment epithelium/Bruch's membrane/choroiocapillaris complex. Mol Aspects Med 2012;33:295–317.

Footnotes and Financial Disclosures

Originally received: March 27, 2013.
Final revision: August 30, 2013.
Accepted: September 4, 2013.
Available online: October 22, 2013. Manuscript no. 2013-497.

[1] Department of Ophthalmology & Vision Science, University of California San Francisco, San Francisco, California.

[2] Department of Biology, California Institute of Technology, Pasadena, California.

[3] Department of Ophthalmology & Vision Science, University of California Davis, Davis, California.

Financial Disclosure(s):
The author(s) have made the following disclosure(s): D.M.S., J.F., and S.E.F. hold an issued patent on the PV-OCT technology. They also hold founders' shares in a company with an interest in the technology. The remaining authors have no conflict of interest.

Supported by the National Eye Institute (EY 014743), Research to Prevent Blindness, Beckman Institute, That Man May See Foundation, and Howard Hughes Medical Institute Med-into-Grad Initiative (56006769). The sponsors and funding agencies had no role in the design or conduct of this research.

Correspondence:
Daniel M. Schwartz, MD, Box 0730, University of California, San Francisco, CA 94143. E-mail: danschwartz7@gmail.com.